Reactivity of Copper(II) Hydroxides and Copper(II) Alkoxides for Cleaving an Activated Phosphate Diester

Mary Jane Young, Daphne Wahnon, Rosemary C. Hynes, and Jik Chin*

Contribution from the Department of Chemistry, McGill University, Montreal, Canada H3A 2K6

Received February 14, 1995[⊗]

Abstract: Two new copper(II) chloride complexes of *N*-(2-hydroxyethyl)bis(pyridylmethyl)amine (CuL_2) and *N*-(3-hydroxypropyl)bis(pyridylmethyl)amine (CuL_3) have been synthesized and characterized. The reactivities of CuL_2 and CuL_3 for cleaving bis(2,4-dinitrophenyl) phosphate (BDNPP) have been compared to that of copper(II) chloride complex of bis(pyridylmethyl)amine (CuL_1). The copper complex with the hydroxypropyl group (CuL_3) cleaves the phosphate diester by transesterification while the complex with the hydroxyethyl group (CuL_2) or the complex without any pendant alcohol groups (CuL_1) cleaves it by hydrolysis. Furthermore, CuL_3 ($k = 7.2 \times 10^{-1}$ M^{-1} s^{-1} at 25 °C, pH 8.8) is about two orders of magnitude more reactive than CuL_2 ($k = 9.5 \times 10^{-3}$ M^{-1} s^{-1}) and CuL_1 ($k = 2.0 \times 10^{-2}$ M^{-1} s^{-1}) for cleaving the diester. The differences in the mechanisms and the reactivities are explained in terms of the differences in the structures of the three copper complexes. Crystal structures of $[(L_1')Cu(OP(O)(OCH_3)_2)(HOCH_3)]Cl$ and $[(L_2')Cu(Cl)]Cl$ have been determined as structural models of CuL_1 and CuL_2, respectively (L_1' = bis(2-benzimidazolylmethyl)amine; L_2' = *N*-(2-hydroxyethyl)bis(2-benzimidazolylmethyl)amine).

Metal hydroxides and metal alkoxides play important roles in hydrolytic metalloenzymes. Metal hydroxides have been implicated in carbonic anhydrase catalyzed hydration of carbon dioxide[1] as well as in carboxypeptidase catalyzed hydrolysis of amides.[2] On the basis of crystallographic data, it has been suggested that the mechanism for alkaline phosphatase catalyzed hydrolysis of phosphate monoesters may involve nucleophilic attack of the phosphate by a zinc coordinated serine hydroxyl group at the active site of the enzyme.[3] A metal alkoxide group may also play an important role in *Tetrahymena* ribozyme catalyzed transesterification of RNA.[4]

There have been numerous model studies that have demonstrated the efficiency of simple metal hydroxides for hydrating carbon dioxide[5] and nitriles,[6] as well as hydrolyzing carboxyl esters,[7] amides,[8] and phosphate esters.[9] In contrast there have been only a few model studies on metal alkoxides. In an elegant recent study, Kimura *et* al.[10] compared the reactivities of zinc hydroxide and zinc alkoxide complexes. Although the zinc complexes were not active for cleaving phosphate esters, the zinc alkoxide was found to be about four times more reactive than the zinc hydroxide for hydrolyzing *p*-nitrophenyl acetate. Here we compare the reactivities and mechanisms of Cu(II) complexes of L_1 (bis(pyridylmethyl)amine),[11] L_2 (*N*-(2-hydroxyethyl)bis(pyridylmethyl)amine), and L_3 (*N*-(3-hydroxypropyl)bis(pyridylmethyl)amine) for cleaving bis(2,4-dinitrophenyl) phosphate (BDNPP).

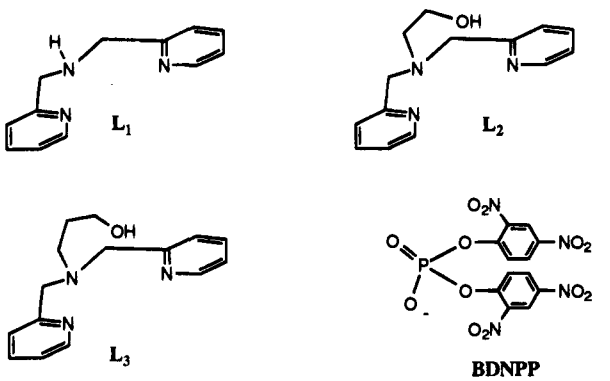

Results and Discussion

For many years, activated phosphate esters with good leaving groups have been used as models of biologically relevant,

[⊗] Abstract published in *Advance ACS Abstracts,* August 15, 1995.

(1) (a) Eriksson, A. E.; Jones, T. A.; Liljas, A. *Proteins: Struct. Funct. Gen.* **1988**, *4*, 274−282. (b) Nair, S. K.; Christianson, D. W. *J. Am. Chem. Soc.* **1991**, *113*, 9455−9458.

(2) Christianson, D. W.; Lipscomb, W. N. *Acc. Chem. Res.* **1989**, *22*, 62−69 and references therein.

(3) Kim, E. E.; Wyckoff, H. W. *J. Mol. Biol.* **1991**, *218*, 449−464.

(4) Steitz, T. A.; Steitz, J. A. *Proc. Natl. Acad. Sci. U.S.A.* **1993**, *90*, 6498−6502.

(5) (a) Woolley, P. *J. Chem. Soc., Perkin Trans. 2* **1977**, 318−324. (b) Tang, C. C.; Davalian, D.; Huang, P.; Breslow, R. *J. Am. Chem. Soc.* **1978**, *100*, 3918−3922. (c) Brown, R. S.; Salmon, D.; Curtis, N. J.; Kusuma, S. *J. Am. Chem. Soc.* **1982**, *104*, 3188−3194. (d) Koike, T.; Kimura, E.; Nakamura, I.; Hashimoto, Y.; Shiro, M. *J. Am. Chem. Soc.* **1992**, *114*, 7338−7345.

(6) (a) Breslow, R.; Fairweather, R.; Keana, J. *J. Am. Chem. Soc.* **1967**, *89*, 2135−2138. (b) Chin, J.; Kim, J. H. *Angew. Chem., Int. Ed. Engl.* **1990**, *29*, 523−525. (c) Kim, J. H.; Britten, J.; Chin, J. *J. Am. Chem. Soc.* **1993**, *115*, 3618−3622.

(7) (a) Buckingham, D. A.; Foster, D. M.; Sargeson, A. M. *J. Am. Chem. Soc.* **1969**, *91*, 4102−4112. (b) Wells, M. A.; Bruice, T. C. *J. Am. Chem. Soc.* **1977**, *99*, 5341−5356. (c) Chin, J.; Jubian, V. *J. Chem. Soc., Chem. Commun.* **1989**, 839−841. (d) Chin, J.; Banaszczyk, M. *J. Am. Chem. Soc.* **1989**, *111*, 2724−2726.

(8) (a) Sutton, P. A.; Buckingham, D. A. *Acc. Chem. Res.* **1987**, *20*, 357−364. (b) Groves, J. T.; Baron, L. A. *J. Am. Chem. Soc.* **1989**, *111*, 5442−5448. (c) Chin, J.; Jubian, V.; Mrejen, K. *J. Chem. Soc., Chem. Commun.* **1990**, 1326−1328. (d) Takasaki, B. K; Kim, J. H.; Rubin, E.; Chin, J. *J. Am. Chem. Soc.* **1993**, *115*, 1157−1159.

(9) (a) Chin, J.; Banaszcyk, M.; Jubian, V.; Zou, X. *J. Am. Chem. Soc.* **1989**, *111*, 186−190. (b) Chin, J. *Acc. Chem. Res.* **1991**, *24*, 145−152. (c) Kim, J. H.; Chin, J. *J. Am. Chem. Soc.* **1992**, *114*, 9792−9795. (d) Connolly, J. A.; Banaszczyk, M.; Hynes, R. C.; Chin, J. *Inorg. Chem.* **1994**, *33*, 665−669. (e) Norman, P. R.; Cornelius, R. D. *J. Am. Chem. Soc.* **1982**, *104*, 2356−2361. (f) Jones, D. R.; Lindoy, L. F.; Sargeson, A. M. *J. Am. Chem. Soc.* **1983**, *105*, 7327−7336. (g) Milburn, R. M.; Gautam-Basak, M.; Tribolet, R.; Sigel, H. *J. Am. Chem. Soc.* **1985**, *107*, 3315−3321. (h) Jones, D. R.; Lindoy, L. F.; Sargeson, A. M. *J. Am. Chem. Soc.* **1984**, *106*, 7807−7819.

(10) Kimura, E.; Nakmura, I.; Koike, T.; Shionoya, M.; Kodama, Y.; Ikeda, T.; Shiro, M. *J. Am. Chem. Soc.* **1994**, *116*, 4764−4771. While this manuscript was under review an interesting communication on Zn(II) alkoxide promoted cleavage of a phosphate triester has been reported: Kady, I. O.; Tan, B.; Ho, Z.; Scarborough, T. *J. Chem. Soc., Chem. Commun.* **1995**, 1137−1138.

(11) Sigel, H.; Hofstetter, F.; Marin, R. B.; Milburn, R. M.; Scheller-Krattiger, V.; Scheller, K. H. *J. Am. Chem. Soc.* **1984**, *106*, 7935−7946.

0002-7863/95/1517-9441$09.00/0

Scheme 1

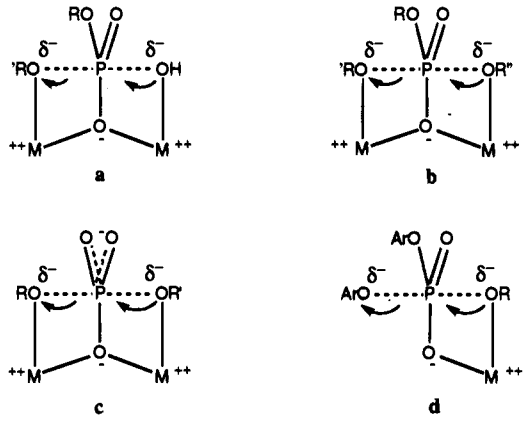

unactivated phosphate esters with poor leaving groups. In some cases activated phosphate esters are good models of unactivated phosphate esters while in other cases they are not. For example, $[(cyclen)Co(OH_2)_2]^{3+}$ provides comparable rate-accelerations for hydrolyzing BNPP[9a] and dimethyl phosphate[9c] while $[(terpy)Cu(OH_2)]^{2+}$ provides a much greater rate-acceleration for hydrolyzing 2′,3′-cyclic AMP than for hydrolyzing BNPP (cyclen: 1,4,7,10-tetraazacyclododecane; terpy: terpyridyl).[12] Although activated phosphate diesters with good leaving groups may not always be good models of unactivated phosphate diesters with poor leaving groups, it is nevertheless important to study hydrolysis of activated phosphate diesters. It has been proposed[9] that in a number of phosphodiesterase (e.g. 3′-5′ exonuclease,[13] RNase H from HIV reverse transcriptase,[14] P1 nuclease,[15] phospholipase C[16] catalyzed hydrolysis) reactions the mechanism involves coordination of the leaving group oxygen to a metal ion (Scheme 1a). Similar mechanisms have been proposed for the *Tetrahymena* ribozyme[17] catalyzed transesterification reaction (Scheme 1, **b**) and alkaline phosphatase[3] catalyzed hydrolysis of phosphate monoesters (Scheme 1, **c**). Mechanisms **a**, **b**, and **c** in Scheme 1 all involve coordination of the leaving group oxygen to a metal ion which converts the poor leaving group into a good one. Furthermore, the mechanisms **b** and **c** in Scheme 1 involve metal alkoxides as nucleophiles. We were interested in finding out if simple metal alkoxides could be made to cleave phosphate esters with good leaving groups by transesterification (Scheme 1, **a**).

Structure. In water the copper(II) chloride complexes of L_1, L_2, and L_3 should all form the square pyramidal dicationic species CuL_1, CuL_2, and CuL_3, respectively. The solvent water molecules are expected to reversibly displace the coordinated pendant alcohol groups in CuL_2 and CuL_3 to varying degrees.

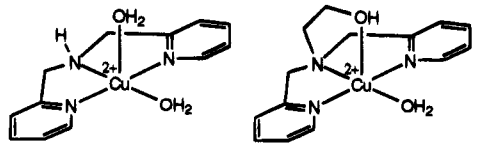

CuL_1 CuL_2

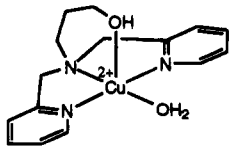

CuL_3

In order to gain some insight into the structures of CuL_1, CuL_2, and CuL_3 we determined the crystal structures of two of their analogs. Bis(2-benzimidazolylmethyl)amine (L_1') and *N*-(2-hydroxyethyl)bis(2-benzimidazolylmethyl)amine (L_2') were synthesized as analogs of L_1 and L_2, respectively. The pyridine groups in L_1 and L_2 are replaced with benzimidazole groups in the two analogs. Crystallographic studies show that $[(L_1')Cu(OP(O)(OCH_3)_2)(HOCH_3)]Cl$ and $[(L_2')Cu(Cl)]Cl$ (abbreviated as $CuL_1'(P)$ and CuL_2', respectively) are square pyramidal in

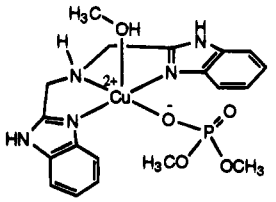

$CuL_1'(P)$

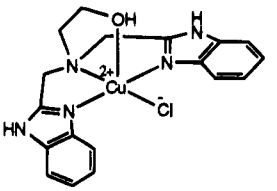

CuL_2'

structure with the alcohol groups coordinated at the apical position. The structures of $CuL_1'(P)$ and CuL_2' are shown in Figures 1 and 2. Crystallographic data and selected bond distances and angles for the two analogs are listed in Tables 1–3.

Titration. Potentiometric titration of CuL_1, CuL_2, and CuL_3 gave one titratable proton each with p*K*(a) values of 8.8, 8.8, and 8.7, respectively. It is not clear whether the observed p*K*(a) values are due to the metal bound alcohol groups or the metal bound water molecules. However, the constancy of the pK_a values suggests that the titratable protons in the three complexes are from the coordinated water molecules at the equatorial position. The coordinated water molecules at the equatorial position should be more acidic than the coordinated water molecules or alcohol groups at the apical position since the equatorial water-to-copper bond lengths are expected to be shorter than the apical water-to-copper or alcohol-to-copper bond lengths.[18] For example, the apical chloride-to-copper bond length in CuL_1' (2.60 Å) is significantly longer than the equatorial chloride-to-copper bond length (2.26 Å) in the same complex.[19]

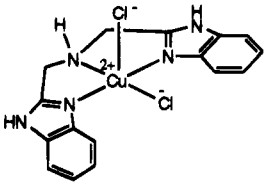

CuL_1'

Cleavage of Phosphate Diesters. It is well-known that *cis*-diaqua metal complexes efficiently hydrolyze phosphate di-

(12) Bashkin, J. K.; Jenkins, L. A. *J. Chem. Soc., Dalton Trans.* **1993**, 3631–3632.
(13) Beese, L. S.; Steitz, T. A. *EMBO J.* **1991**, *10*, 25–33.
(14) Davies, J. F., II; Hostomska, Z.; Hostomsky, Z.; Jordan, S. R.; Matthews, D. A. *Science* **1991**, *252*, 88–95.
(15) Volbeda, A.; Lahm, A.; Sakiyama, F.; Suck, D. *EMBO J.* **1991**, *10*, 1607–1618.
(16) Hough, E.; Hansen, L. K.; Birkness, B.; Jynge, K.; Hansen, S.; Hordvik, A.; Little, C.; Dodson, E.; Derewenda, Z. *Nature* **1989**, *338*, 357–360.
(17) Piccirilli, J. A.; Vyle, J. S.; Caruthers, M. H.; Cech, T. R. *Nature* **1993**, *361*, 85–88.
(18) (a) Uma, R.; Viswanathan, R.; Palaniandavar, M.; Lakshminarayanan, M. *J. Chem. Soc., Dalton Trans.* **1994**, 1219–1226. (b) Karlin, K. D.; Hayes, J. C.; Juen, S.; Hutchinson, J. P.; Zubieta, J. *Inorg. Chem.* **1982**, *21*, 4106–4108. (c) Oberhausen, K. J.; O'Brien, R. J.; Richardson, J. F.; Buchanan, R. M. *Inorg. Chim. Acta* **1990**, *173*, 145–154. (d) Nishida, Y.; Takahashi, K. *J. Chem. Soc., Dalton Trans.* **1988**, 691–699.
(19) Wahnon, D.; Hynes, R. C.; Chin, J. *J. Chem. Soc., Chem. Commun.* **1994**, 1441–1442.

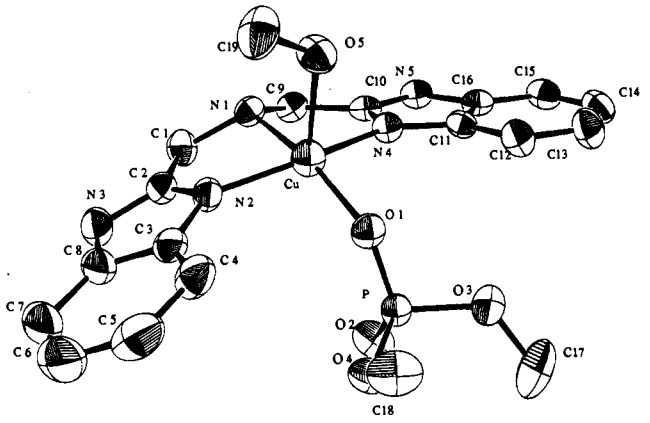

Figure 1. Structure of $CuL_1'(P)$ showing 50% probability ellipsoids.

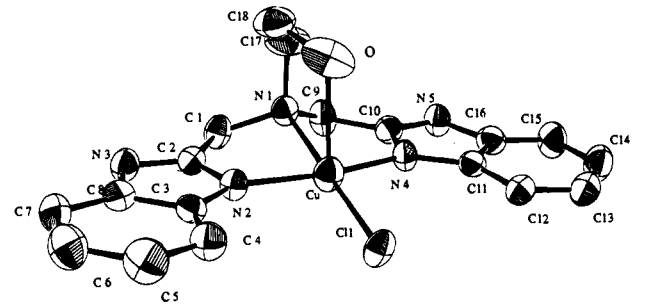

Figure 2. Structure of CuL_2' showing 50% probability ellipsoids.

Table 1. Crystallographic Data for $CuL_1'(P)$ and CuL_2' [a]

molecular formula	$C_{19}H_{25}N_5O_9PClCu$	$C_{18}H_{25}N_5O_4Cl_2Cu$
mol wt	597.40	508.89
cryst system	triclinic	monoclinic
space group	$P\bar{1}$	$A2/a$
a (Å)	7.2573(11)	14.324(4)
b (Å)	12.7707(17)	17.158(5)
c (Å)	13.3686(20)	18.712(5)
α (deg)	85.213(12)	
β (deg)	80.009(12)	109.305(18)
γ (deg)	82.413(12)	
V (Å^3)	1207.2(3)	4340.3(19)
Z	2	8
ϱ_{calc} (g/cm^3)	1.643	1.561
cryst dimens (mm)	0.40 × 0.123 × 0.20	0.40 × 0.20 × 0.20
temp (°C)	20 ± 1	20 ± 1
μ (mm^{-1})	3.47	4.02
h, k, l limits	−7 to 7, 0 to 13, −14 to 14	−15 to 14, 0 to 18, 0 to 19
2θ range (deg)	5 to 110	5 to 110
$F(000)$	614	2104
no. of data collected	3337	2879
no. of unique data	3045	2745
no. of data with $I > 2.5\sigma(I)$	2808	2382
no. of variables	353	280
weight modifier "k"	5.0×10^{-4}	5.0×10^{-4}
R	0.047	0.059
R_w	0.063	0.069
R_{int} (no of reflcns)	0.016 (584)	0.021 (168)
secondary ext. coef	0.19(3)	
goodness of fit	4.62	3.59
last ΔF (e/Å^3)	0.32 to −0.64	0.84 to −0.68

[a] $R = \Sigma(F_o - F_c)/\Sigma F_o$. $R_w = \{(\Sigma[w(F_o - F_c)^2])/\Sigma wF_o^2\}$. $w = (1/\sigma^2F_o) + kF_o^2$. GoF = $\{(\Sigma[w(F_o - F_c)^2])/$(no. of reflections − no. of parameters)$\}^{1/2}$.

esters.[9] It has been proposed that the mechanism of the hydrolysis reaction involves the coordination of the phosphate diester to the metal (M) complex followed by intramolecular metal hydroxide attack on the coordinated phosphate (Scheme 2).[9] It is the *cis*-aqua hydroxy form of the metal complex that is the active species for hydrolyzing phosphate diesters (Scheme 2). *cis*-Aqua hydroxy metal complexes may also form inactive dimers at high concentrations (Scheme 3).[20] A term for the overall rate constant (k_{obs}) for *cis*-diaqua metal complex catalyzed hydrolysis of phosphate diesters according to the mechanism in Scheme 3 is shown in eq 1 where $[Cu]_T$ represents the total copper complex concentration and [H] represents the proton concentration.

Table 2. Selected Bond Distances (Å) and Angles (deg) for $CuL_1'(P)$

	Bond Distances		
Cu−O(1)	1.970(3)	Cu−N(1)	2.101(4)
Cu−O(5)	2.241(4)	Cu−N(2)	1.966(4)
Cu−N(4)	1.960(4)		
	Bond Angles		
O(1)−Cu−O(5)	95.70(14)	O(5)−Cu−N(2)	98.14(16)
O(1)−Cu−N(1)	164.95(16)	O(5)−Cu−N(4)	95.42(15)
O(1)−Cu−N(2)	96.17(16)	N(1)−Cu−N(2)	81.39(17)
O(1)−Cu−N(4)	97.76(15)	N(1)−Cu−N(4)	81.25(16)
O(5)−Cu−N(1)	99.34(15)	N(2)−Cu−N(4)	159.46(17)

Table 3. Selected Bond Distances (Å) and Angles (deg) for CuL_2'

	Bond Distances		
Cu−Cl	2.2346(20)	Cu−N(1)	2.116(6)
Cu−O	2.509(6)	Cu−N(2)	1.942(6)
		Cu−N(4)	1.956(6)
	Bond Angles		
Cl−Cu−O	102.65(7)	O−Cu−N(2)	86.00(23)
Cl−Cu−N(1)	179.05(18)	O−Cu−N(4)	96.91(23)
Cl−Cu−N(2)	97.90(17)	N(1)−Cu−N(2)	82.09(23)
Cl−Cu−N(4)	97.95(17)	N(1)−Cu−N(4)	81.96(23)
O−Cu−N(1)	78.20(21)	N(2)−Cu−N(4)	162.82(23)

Scheme 2

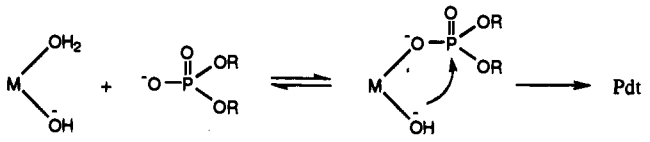

Scheme 3

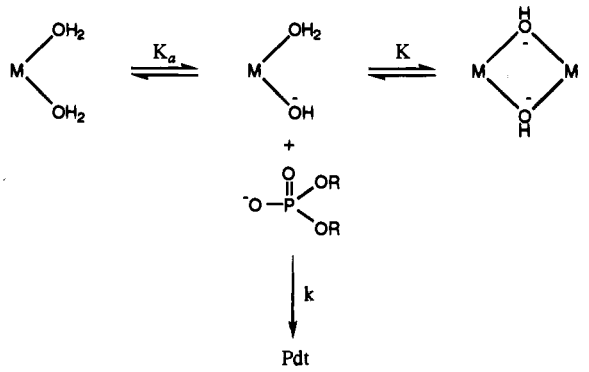

$$k_{obs} = k\{((1 + [H]/K_a)^2 + 8K[Cu]_T)^{1/2} - (1 + [H]/K_a)\}/4K \quad (1)$$

Equation 1 should also be applicable for *cis*-aqua alcohol metal complexes since they too may cleave phosphate diesters and form dimers with bridging alkoxides or hydroxides.

The Cu(II) complexes CuL_1, CuL_2, and CuL_3 all cleave BDNPP with concomitant release of 1 equiv of 2,4-dinitrophenol. All three complex solutions (10 mM, pH 10) did not lose

(20) (a) Courtney, R. C.; Gustafson, R. L.; Chaberek, S., Jr.; Martell, A. E. *J. Am. Chem. Soc.* **1959**, *81*, 519−524. (b) Gustafson, R. L.; Martell, A. E. *J. Am. Chem. Soc.* **1959**, *81*, 525−529. (c) Burstyn, J. N.; Deal, K. A. *Inorg. Chem.* **1993**, *32*, 3585−3586.

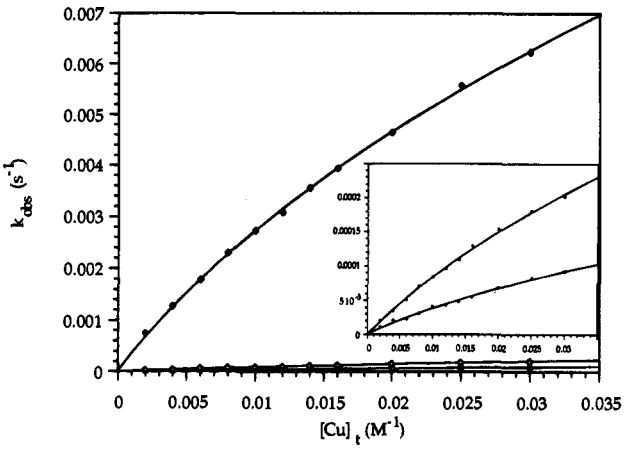

Figure 3. Dependence of the rate of cleavage of BDNPP (10^{-5} M) on the concentrations of CuL_1 (middle), CuL_2 (bottom), and CuL_3 (top) at 25 °C, pH 8.8 (inset: expanded scale for CuL_1 and CuL_2).

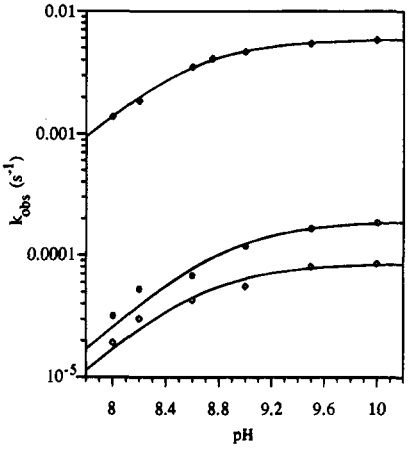

Figure 4. Rate–pH profile for cleavage of BDNPP (10^{-5} M) with 10 mM solutions of CuL_1 (middle), CuL_2 (bottom), and CuL_3 (top) at 25 °C.

activity for cleaving BDNPP to any observable extent for 1.5 h. The rate of CuL_1, CuL_2, and CuL_3 promoted cleavage of BDNPP was monitored by following the increase in the visible absorbance at 400 nm due to the release of 2,4-dinitrophenolate. At pH 8.8, the rate of cleavage of BDNPP initially increases linearly with increase in the concentrations of the metal complexes but gradually deviates down from linearity (Figure 3). The equilibrium constants (K) for apparent dimerization of the mono-cationic forms of CuL_1, CuL_2, and CuL_3 obtained by fitting the concentration–rate profiles according to eq 1 are 5×10^1, 6×10^1, and 8×10^1 M^{-1}, respectively. The k values (Scheme 3) for CuL_1, CuL_2, and CuL_3 are 2.0×10^{-2}, 9.5×10^{-3}, and 7.2×10^{-1} M^{-1} s^{-1}, respectively.

The rates of CuL_1, CuL_2, and CuL_3 promoted cleavage of BDNPP increase with increase in the solution pH but level off above the pK_a of the copper bound water molecules (Figure 4). The pH–rate profiles were fit according to eq 1 with the K values (Scheme 3) fixed above and $[Cu]_t = 10$ mM. The best fit gave pK_a values of 9.0, 8.9, and 8.8 and k values of 3.0×10^{-2}, 1.4×10^{-2}, and 1.1 M^{-1} s^{-1} for CuL_1, CuL_2, and CuL_3 respectively. The pK_a values obtained from the pH–rate profiles are in reasonably good agreement with those obtained from potentiometric titrations. The k values (Scheme 3) obtained from the pH–rate profiles are also in agreement with those obtained from the concentration–rate profiles.

Covalent Intermediate. Interestingly, CuL_3 is almost two orders of magnitude more reactive than CuL_1 or CuL_2 for cleaving BDNPP. Furthermore, HPLC analysis (Figure 5)

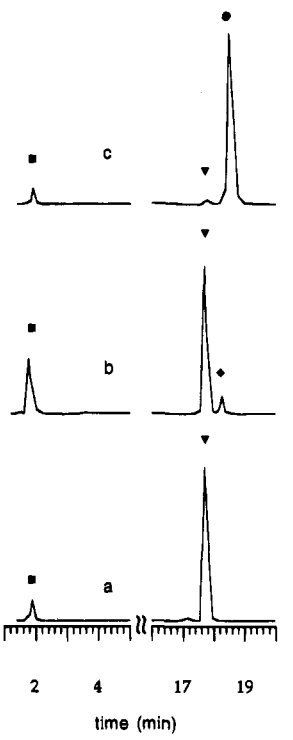

Figure 5. HPLC analysis for cleavage of BDNPP with (a) CuL_1, (b) CuL_2, and (c) CuL_3: (■) 2,4-dinitrophenyl phosphate; (▼) BDNPP; (◆) L_2-P; (●) L_3-P.

Scheme 4

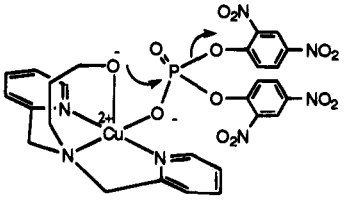

indicates that CuL_1 cleaves BDNPP hydrolytically to give the phosphate monoester (2,4-dinitrophenyl phosphate) and 2,4-dinitrophenol while CuL_2 and CuL_3 cleave the diester by hydrolysis and by transesterification to give the phosphate monoester, 2,4-dinitrophenol, and the transesterified products (L_2-P and L_3-P). The transesterified products were first detected by HPLC, isolated by preparative chromatography, and characterized by ^1H and ^{31}P NMR as well as by HPLC and mass spectrometry. The HPLC analyses (Figure 5) indicate that the

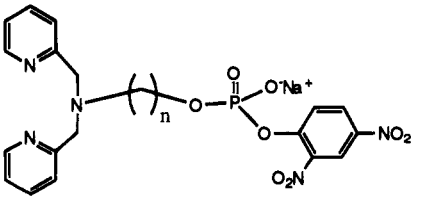

n = 2 : L_2-P
n = 3 : L_3-P

Cu(II) complex with the hydroxypropyl group (CuL_3) cleaves BDNPP predominantly by transesterification (95% ± 3%) whereas the Cu(II) complex with the hydroxyethyl group (CuL_2) cleaves the diester predominantly by hydrolysis (90% ± 2%).

Mechanism. We propose that CuL_3 cleaves BDNPP by first coordinating the phosphate diester followed by intramolecular metal alkoxide attack (Scheme 4). This imples that the aqua alkoxy form of the metal complex rather than the thermody-

Scheme 5

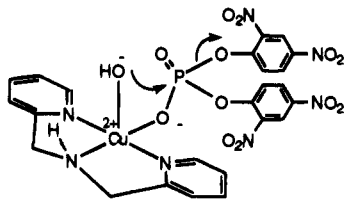

namically more stable hydroxy alcohol form of the metal complex is the active species for cleaving the phosphate diester. Since the ratio of the concentration of the aqua alkoxy form of the metal complex to that of the hydroxy alcohol form of the metal complex is independent of pH, and pH−rate profile (Figure 4) cannot be used to identify the active species. The structure in Scheme 4 may be compared with the crystal structure of CuL_1'-**P**. In both structures, a phosphate diester is coordinated at the equatorial position and an alkoxide or an alcohol is coordinated at the apical position. The reactivity of CuL_3 should depend on its overall structure. In particular, the nucleophilic attack by the metal alkoxide on the coordinated phosphate diester (Scheme 4) should be facilitated by a decrease in the O−Cu−O bond angle. The propyl group in CuL_3 should expand the N(alkylamine)−Cu−O bond angle thereby decreasing the O−Cu−O bond angle.

Similar to the mechanism for CuL_3 promoted cleavage of BDNPP, CuL_1 may hydrolyze the diester by intramolecular metal hydroxide attack on the coordinated phosphate diester (Scheme 5). The greater reactivity of CuL_3 compared to that of CuL_1 may be due to the greater value of the O−Cu−O bond angle in the latter complex. In a related study, it has been shown that the reactivity of *cis*-diaqua tetraamine Co(III) complexes for hydrolyzing phosphate diesters increases with decreasing O−Co−O bond angle which can be achieved by increasing the N−Co−N bond angle opposite the O−Co−O bond angle.[9,21]

When the propyl bridging group in CuL_3 is replaced with the ethyl bridging group (CuL_2) the reactivity of the metal complex for cleaving BDNPP decreases by about two orders of magnitude. It appears that the metal alkoxide of CuL_2 cannot easily reach the phosphate due to the increased O−Cu−O bond angle and the decreased N(alkyl amine)−Cu−O bond angle. Indeed the O−Cu−Cl bond angle in CuL_2' (102.75°) is significantly greater than the O−Cu−O bond angle in CuL_1'(**P**) (95.70°) presumably because the N(alkyl amine)−Cu−O bond angle in CuL_2' (78.20°) is much smaller than that in CuL_1'(**P**) (99.34°). The Cu(II) complex **CuL_2** is about two orders of magnitude less reactive than CuL_3 and about half as reactive as CuL_1. Furthermore, CuL_2 cleaves the diester predominantly by hydrolysis rather than by transesterification. It appears that the more active form of CuL_2 is formed by displacement of the coordinated alkoxide by hydroxide. The metal hydroxide can then attack the coordinated phosphate diester much like with CuL_1 (Scheme 5). Although we cannot rule out the possibility that the metal hydroxide or metal alkoxide in CuL_1 or CuL_2 may be acting as an intramolecular general base catalyst, it seems unlikely that the mechanistic role of the metal hydroxide in CuL_1 would be different from the mechanistic role of the metal alkoxide in CuL_3.

In summary, three Cu(II) complexes, CuL_1, CuL_2, and CuL_3, have been prepared in order to investigate the reactivities of metal alkoxides and metal hydroxides for cleaving an activated phosphate diester. The Cu(II) complex with the hydroxypropyl group (CuL_3) is about a hundred times more reactive than the Cu(II) complex with the hydroxyethyl group (CuL_2) and over thirty times more reactive than the Cu(II) complex without any pendant alcohol groups (CuL_1). Interestingly, HPLC analyses provide direct evidence that the three complexes do not cleave BDNPP by the same mechanism. CuL_1 cleaves the diester by direct hydrolysis. CuL_2 cleaves the diester predominantly by hydrolysis but some transesterification can also be detected. CuL_3 cleaves the diester mainly by transesterification. Based on crystallographic data of two analogs (CuL_1'(**P**) and CuL_2') we have proposed that the differences in the reactivities and mechanisms of the three complexes can be explained in terms of the differences in their structures. These results demonstrate how subtle changes in the structure of simple metal complexes can influence their reactivity. A possible advantage for an enzyme to employ a metal alkoxide instead of a metal hydroxide may be the preferential positioning of the nucleophile. In conclusion, we have shown that a simple metal complex with a pendant alcohol group can efficiently cleave a phosphate diester by transesterification much as has been proposed for alkaline phosphatase catalyzed cleavage of phosphate monoesters and *Tetrahymena* ribozyme catalyzed transesterification reaction.

Experimental Section

General Information. ^{1}H NMR (299.3 MHz), ^{13}C NMR (75.4 MHz), and ^{31}P NMR (121.4 MHz) spectra were obtained on a Varian XL-300 FT spectrophotometer. ^{1}H NMR (199.975 MHz) and ^{13}C NMR (50.289 MHz) were obtained on a Varian Gemini 200 spectrophotometer. Kinetic studies were carried out by UV−vis methods with a Hewlett Packard 8452 diode array spectrophotometer equipped with a Lauda RM6 thermostat. High-performance liquid chromatography (HPLC) was performed on a HP1090 using a 2.1 mm × 100 mm Hypersil ODS C-18 reversed-phase column. Titrations of the metal complexes were carried out with a Radiometer RTS822 automatic titrator. Infrared spectra were obtained on a Bruker IFS FTIR spectrophotometer and an Analect AOS spectrophotometer. All mass spectra were obtained on a KRATOS MS25RFA spectrometer.

Materials. All reagents unless otherwise indicated were of analytical grade and were used without further purification. Bis(pyridylmethyl)-amine (L_1),[22] [(L_1)$CuCl_2$],[11,23] *N*-(2-hydroxyethyl)bis(2-pyridylmethyl)-amine (L_2),[24] bis(2-benzimidazolylmethyl)amine (L_1'),[18d] 2,4-dinitrophenyl phosphate,[25] and bis(2,4-dinitrophenyl) phosphate (BDNPP)[26] were prepared by previously reported methods.

***N*-(3-Hydroxypropyl)bis(2-pyridylmethyl)amine (L_3).** 2-Pyridinecarboxaldehyde (0.09 mol), 3-aminopropanol (0.045 mol), and acetic acid (0.09 mol) were mixed together in dry THF. Sodium triacetoxyborohydride (0.12 mol) was added to the above solution and stirred at room temperature for 48 h under nitrogen. After removing the solvent *in vacuo*, the product was dissolved in CH_2Cl_2 and washed with an aqueous solution saturated with sodium bicarbonate. The product was distilled to give a pale yellow oil (yield 58%; bp 130 °C, 0.03 mmHg). IR (neat) 3200−3500, 2950, 2809, 1593, 1571, 1474, 1436, 1050 cm^{-1}. ^{1}H NMR (299.3 MHz, $CDCl_3$, (TMS)) δ 1.82 (2H, m), 2.78 (2H, t), 3.73 (2H, t), 3.84 (4H, s), 7.17 (2H, t), 7.41 (2H, d), 7.64 (2H, t), 8.55 (2H, d). ^{13}C NMR (75.4 MHz, $CDCl_3$, dioxane (66.7 ppm)) δ 28.5, 52.4, 59.6, 61.9, 121.7, 122.7, 136.2, 148.7, 158.6. MS (EI, ion source 200 °C, 70 eV, direct inlet 100 °C), [*m/z* (relative intensity)]: 257 ($M^{\bullet+}$, 2), 165 (74), 135 (32), 93 (100).

N-(2-hydroxyethyl)bis(2-benzimidazolylmethyl)amine (L_2'). *N*-(2-Hydroxyethyl)iminodiacetic acid (2.0 g, 0.01 mol) and 1,2-diaminobenzene (2.44 g, 0.023 mol) were ground into a fine powder with a mortar and pestle and heated to 170−180 °C for 1 h until no further steam was detected. After cooling to room temperature, 100 mL of

(21) Connolly, J.; Kim, J. H.; Banaszczyk, M.; Drouin, M.; Chin, J. *Inorg. Chem.* **1995**, *34*, 1094−1099.

(22) Larsen, S.; Michelson, K.; Pedersen, E. *Acta Chem. Scand A* **1986**, *40*, 63−76.

(23) Romary, J. K.; Barger, J. D.; Bunds, J. E. *Inorg. Chem.* **1968**, *7*, 1142−1145.

(24) Groves, J. T.; Kady, I. O. *Inorg. Chem.* **1993**, *32*, 3868−3872.

(25) Rawji, G.; Milburn, R. M. *J. Org. Chem.* **1981**, *46*, 1205−1206.

(26) Bunton, C. A.; Farber, S. J. *J. Org. Chem.* **1969**, *34*, 767−772.

concentrated hydrochloric acid was added to dissolve the resulting dark glassy substance. A blue precipitate which formed after 5 min of sonication was filtered and washed with acetone and immediately dissolved in 100 mL of water. The pink-white precipitate which formed upon basification of the solution with concentrated ammonium hydroxide was recrystallized from hot acetone to give 2.1 g of an off-white precipitate (yield 58%). ^{1}H NMR (200 MHz, CD_3OD) δ 2.76 (2H, t), 3.66 (2H, t), 4.06 (4H, s), 7.22 (4H, m), 7.54 (4H, m). ^{13}C NMR (75.4 MHz, CD_3OD) δ 53.73, 57.68, 60.41, 115.73, 123.71, 139.27, 154.04. MS (EI, ion source 350 °C, 70 eV, direct inlet 100 °C), [*m/z* (relative intensity)]: 321 ($M^{\bullet+}$, 0.06), 189 (27), 160 (51.7), 132 (100, 131 (58.8), 119 (20.4).

[(L_2)$CuCl_2$]. A solution of $CuCl_2$ (1.5 mmol) in 10 mL of ethanol was added to a solution of L_2 (1.5 mmol) in 10 mL of ethanol. After 2 h the total volume of the mixture was reduced to 10 mL. A blue precipitate that appeared after addition of 5 mL of ether was filtered and washed with cold ethanol. The complex was dried overnight *in vacuo* (67% yield). IR (neat) 3100−3500, 2960, 2880, 1610, 1570, 1480, 1440, 1380, 1350, 1300, 1290, 1070, 1040, 1030, 990 cm^{-1}. UV/vis (H_2O, pH 6): 254 nm (ϵ = 1.15 × 10^4 cm^{-1} M^{-1}); 678 nm (ϵ = 84 cm^{-1} M^{-1}). Anal. Calcd for $C_{14}H_{17}N_3OCuCl_2$: C, 44.51; H, 4.50; N, 11.12; Cl, 18.77; Cu, 16.82. Found: C, 44.67; H, 4.61; N, 11.03; Cl, 19.06; Cu, 16.51.

[(L_3)$CuCl_2$]. A solution of $CuCl_2$ (4.5 mmol) in 10 mL of ethanol was added to a solution of L_3 (4.5 mmol) in 10 mL of ethanol. A blue precipitate that formed within minutes was filtered and washed with cold ethanol. The complex was dried overnight *in vacuo* (64% yield). IR (neat) 3100−3500, 3070, 2870, 1610, 1570, 1480, 1440, 1380, 1300, 1280, 1100, 1050, 975 cm^{-1}. UV/vis (H_2O, pH 6): 254 nm (ϵ = 1.34 × 10^4 cm^{-1} M^{-1}); 658 nm (ϵ = 108 cm^{-1} M^{-1}). Anal. Calcd for $C_{15}H_{19}N_3OCuCl_2$: C, 45.99; H, 4.89; N, 10.77; Cl, 18.10; Cu, 16.22. Found: C, 46.06; H, 5.05; N, 10.75; Cl, 18.35; Cu, 16.50.

[(L_1')Cu(OP(O)(OCH_3)$_2$)($HOCH_3$)](ClO_4). The perchlorate salt of CuL_1' ((L_1')Cu(ClO_4)$_2$·2H_2O) was first prepared in 70% yield by mixing L_1' (1 mmol) and Cu(ClO_4)$_2$·H_2O (1 mmol) in methanol (8 mL). Sodium dimethyl phosphate (0.5 mmol) was then added to a methanolic solution (10 mL) of (L_1')Cu(ClO_4)$_2$ (0.5 mmol) to give blue crystals of the product (CuL_1(**P**)) in 5−10 min (58% yield). The blue crystals were washed with cold methanol and dried under vacuum for 6 h.

[(L_2')Cu(Cl)]Cl·3(H_2O). To a stirred solution (0.6 mmol) of $CuCl_2$·2H_2O in 5 mL of ethanol was added dropwise a solution (0.6 mmol) of L_2' in 5 mL of ethanol. The green crystals (CuL_2') which formed after 5−10 min were filtered after stirring for 1 h and washed with cold methanol (48% yield).

Titration. Solutions (3 mL, 15 mM) of CuL_1, CuL_2, and CuL_3 in water (25 °C) were titrated with a 0.1 M NaOH solution. The ionic strength was maintained at 0.1 M with $NaNO_3$.

Kinetics. Hydrolysis of BDNPP was monitored by following the visible absorbance change at 400 nm due to the release of 2,4-dinitrophenolate anion. One equivalent of 2,4-dinitrophenolate was released for each reaction.

The rate constants for CuL_1 and CuL_2 promoted hydrolysis of BDNPP were obtained by the initial rate method. The rate constants for CuL_3 promoted hydrolysis of BDNPP were obtained by fitting the first 3 half-lives of the reaction according to a first-order kinetics equation. In a typical kinetics experiment 5 μL of a freshly prepared BDNPP stock solution in dimethyl sulfoxide (10 mM) was added to a freshly prepared copper complex solution (2 to 30 mM) at 25 °C. The copper complex solutions were buffered with CHES (10 mM, pH 8.6−10) or NEM (10 mM, pH 7−8.2). The pH of the solutions was adjusted using concentrated NaOH or $HClO_4$ solution.

Product Analysis. The products for CuL_1, CuL_2, and CuL_3 promoted cleavage of BDNPP were analyzed by HPLC. In a typical experiment, the metal complex (2.4 × 10^{-4} mol) was reacted with an equivalent amount of BDNPP in water (25 mL) at 22 °C. The pH of the reaction solution was maintained between 8.5 and 9.5 with sodium hydroxide. After 2 to 7 h, EDTA (2.4 × 10^{-3} mol) was added to complex the copper. The reaction mixture was injected (5 μL) onto a C-18 reversed-phase HPLC column (5 μm Hypersil maintained at 40 °C) and eluted for 5 min with $NH_4H_2PO_4$ (0.2 M at pH 5.5) followed by a 0−100% linear gradient of the ammonium phosphate and methanol/water (3/2) solutions over 20 min with a flow rate of 0.5 mL/min. For the cleavage of BDNPP with CuL_1, the HPLC peak (at 254 nm) due to the diester (retention time: 17.9 min) decreased with concomitant increase in the peaks due to the monoester DNPP (1.6 min) and 2,4-dinitrophenol (8.7 min). For the cleavage of the diester with CuL_2 and CuL_3, the decrease in the diester peak was accompanied by an increase in the peaks due to the monoester as well as the transesterified products (L_2-**P**, 18.4 min; L_3-**P**, 18.8 min) and 2,4-dinitrophenol.

Isolation of L_3-P. The above EDTA quenched reaction mixture for the cleavage of BDNPP by CuL_3 was extracted into dichloromethane. After removing the dichloromethane *in vacuo*, the extract was applied onto a 6 cm × 30 cm reversed-phase C-18 column and eluted with methanol/water (1/4) until all of the 2,4-dinitrophenol was removed from the column. A linear gradient up to methanol/water (3/2) was used to elute L_3-**P**. Further purification was performed by extracting L_3-**P** into water from dichloromethane giving a yellow solid upon lyophilization (yield: 26%). HPLC analysis of the yellow solid under the above condition for product analysis gave a single peak with a retention time of 18.8 min. ^{1}H NMR (200 MHz, D_2O, (DSS)): δ 1.96 (2H, m), 2.73 (2H, t), 3.62 (4H, s), 4.03 (2H, m), 7.30 (2H, t), 7.41 (2H, d), 7.62 (1H, d), 7.78 (2H, t), 8.4 (3H, m), 8.80 (1H, d). ^{13}C NMR (50.289 MHz, D_2O, dioxane (66.7 ppm)) δ 27.4, 50.7, 59.5, 65.8, 121.1, 121.9, 122.3, 123.4, 128.63, 137.0, 147.1, 156.58. ^{31}P NMR (121 MHz, D_2O, (trimethyl phosphate)) δ −8.8. MS (FAB, NBA matrix, 7 kV) [*m/z* (relative intensity)]: 679, 0.8% ($C_{21}H_{21}N_5NaO_8P$ + NBA + H)$^+$; 526, 1.5% ($C_{21}H_{21}N_5NaO_8P$ + H)$^+$; 504, 6.2% ($C_{21}H_{23}N_5NaO_8P$)$^+$.

Isolation of L_2-P. L_2-**P** was isolated under the same experimental conditions for isolating L_3-**P**. HPLC analysis of L_2-**P** gave a single peak with a retention time of 18.4 min. ^{1}H NMR (200 MHz, D_2O, (DSS)): δ 2.86 (2H, t), 3.75 (4H, s), 4.12 (2H, m), 7.25 (2H, t), 7.44 (2H, d), 7.72 (3H, m), 8.35 (3H, m), 8.78 (1H, d). ^{13}C NMR (50.289 MHz, D_2O, dioxane (66.7 ppm)) δ 54.0, 59.9, 61.5, 122.0, 122.7, 123.0, 124.4, 129.6, 137.0, 148.0, 156.58. ^{31}P NMR (121 MHz, D_2O, (trimethyl phosphate)) δ −8.8. MS (FAB, NBA matrix, 7 kV) [*m/z* (relative intensity)]: 512, 0.8% ($C_{20}H_{19}N_5NaO_8P$ + H)$^+$; 490, 3.1% ($C_{20}H_{21}N_5NaO_8P$)$^+$.

X-ray Diffraction Studies. The intensity data were collected on a Rigaku AFC6S diffractometer using the ω−2θ scan mode. Graphite-monochromated Cu Kα (1.54056 Å) radiation was used. NRCVAX[27] crystallographic software was used for solution and refinement calculations. The structures were solved by direct methods. Data are summarized in Table 1.

The perchlorate salt of CuL_1'(**P**) ([(L_1')Cu(OP(O)(OCH_3)$_2$)($HOCH_3$)](ClO_4)) was recrystallized at the acetone−hexane interface yielding blue block crystals. Cell dimensions were obtained from 25 reflections with 2θ in the range 70−90°. Data were collected to a maximum 2θ of 110°. The cell is triclinic, space group $P\bar{1}$ with dimensions a = 7.2573(11) Å, b = 12.7707(17) Å, c = 13.3686(20) Å, α = 85.213(12)°, β = 80.009(12)°, γ = 82.413(12)°, and V = 1207.2(3) Å^3, with Z = 2. Absorption corrections were made from 4 ψ scans with transmission factors ranging from 0.376 to 0.525. Hydrogens on N and O were located in a difference map but not refined. Other hydrogens were included in calculated positions. The structure was refined by full-matrix least-squares with all non-hydrogens anisotropic. The final refinement was based on 2808 observed reflections ($I > 2.5\sigma(I)$) and 353 parameters and converged with agreement factors of R = 0.047 and R_w = 0.063. Refinement on $|F|$ with weights based on counting statistics. The perchlorate anion has two orientations, differing by a rotation about the O1−Cl bond with occupancies of 0.6 and 0.4. Selected bond distances (Å) and bond angles (deg) of CuL_1'(**P**) are shown in Table 2.

The chloride salt of CuL_2' ([(L_2')Cu(Cl)]Cl·3(H_2O)) was recrystallized from methanol yielding blue oblong crystals. Cell dimensions were obtained from 25 reflections with 2θ in the range 90−100°. Data were collected to a maximum 2θ of 110.0°. The cell is monoclinic,

(27) Gabe, E. J.; LePage, Y.; Charland, J. P.; Lee, F. L.; White, P. S. *J. Appl. Crystallogr.* **1989**, *22*, 384−387.

space group $A2/a$ with dimensions $a = 14.324(4)$ Å, $b = 17.158(5)$ Å, $c = 18.712(5)$ Å, $\beta = 109.305(18)°$, and $V = 4340.3(19)$ Å^3, with $Z = 8$ and $\varrho_{calc} = 1.564$ g/cm^3. Absorption corrections were made from 4 ψ scans with transmission factors ranging from 0.454 to 0.520. Hydrogens were calculated except those on the solvent water molecules which were omitted. The structure was refined by full-matrix least-squares with all non-hydrogens anisotropic. The final refinement was based on 2382 observed reflections ($I > 2.5\sigma(I)$) and 280 parameters and converged with agreement factors of $R = 0.059$ and $R_w = 0.069$. Refinement on $|F|$ with weights based on counting statistics. C(18) is disordered in two positions with occupancies of 0.35 and 0.65. There are three water molecules per copper. The structure exists as a loosely associated dimer arranged about an inversion center with asymmetric chlorine bridges. The copper of one moiety interacts with the Cl of the other with a Cu−Cl distance of 3.1849(24) Å. Selected bond distances (Å) and bond angles (deg) of CuL_2' are shown in Table 3.

Acknowledgment. We thank Erik Rubin for preliminary studies. Financial support was provided by the Natural Sciences and Engineering Research Council of Canada and the U.S. Army Research Office.

Supporting Information Available: X-ray structural information for the compounds in Table 1 including crystal packing diagram, positional parameters, and interatomic distances and angles (11 pages). This material is contained in many libraries on microfiche, immediately follows this article in the microfilm version of the journal, can be ordered from the ACS, and can be downloaded from the Internet; see any current masthead page for ordering information and Internet access instructions.

JA950524C